Materials & Design 225 (2023) 111597

Contents lists available at ScienceDirect

Materials & Design

journal homepage: www.elsevier.com/locate/matdes

Direct fabrication of arrays of Cu(In,Ga)Se_2 micro solar cells by sputtering for micro-concentrator photovoltaics

Ricardo G. Poeira [a,*], Ana Pérez-Rodríguez [b,1], Aubin J.C. M. Prot [a], Marina Alves [b,c], Phillip J. Dale [a], Sascha Sadewasser [b,*]

[a] Department of Physics and Materials Science, University of Luxembourg, 41, rue du Brill, L-4422 Belvaux, Luxembourg
[b] INL - International Iberian Nanotechnology Laboratory, Av, Mestre José Veiga, s/n, 4715-330 Braga, Portugal
[c] Centre of Physics of Minho and Porto Universities (CF-UM-UP), Azurém Campus, 4800-058 Guimarães, Portugal

HIGHLIGHTS

- We demonstrate a novel material-efficient synthesis of arrays of Cu(In,Ga)Se_2 micro solar cells through lithography, sputtering deposition and reactive-annealing processes.
- Unexpected resist contamination of the Cu-In-Ga precursor island requires a newly introduced pre-annealing step to remove the unwanted resist.
- Surprisingly, constrained Cu-In-Ga selenizes to Cu(In,Ga)Se_2 by not only growing upwards in its hole, but also outwards with non-uniform composition.
- Functional proof of principle Cu(In,Ga)Se_2 micro solar cell arrays were produced with a power conversion efficiency of 1.2%.

GRAPHICAL ABSTRACT

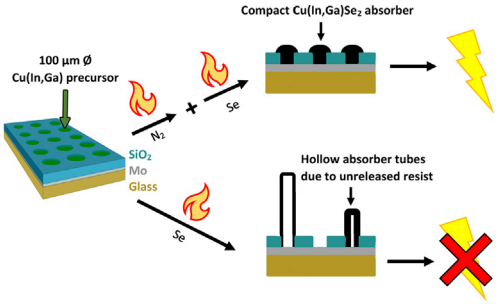

ARTICLE INFO

Article history:
Received 3 October 2022
Revised 3 January 2023
Accepted 3 January 2023
Available online 5 January 2023

Keywords:
Thin-film photovoltaics
Micro-concentrator photovoltaics
Material-efficient synthesis
Cu(In
Ga)Se_2
Sputtering
Micro solar cell array

ABSTRACT

Micro-concentrator photovoltaics combines efficiency boosting light concentration with low electrical losses due to thermally cool sub-millimeter sized solar cells. Thin-film Cu(In,Ga)Se_2 absorber layers do not suffer from edge recombination enabling miniaturization to the micrometer size, which allows for considerable material saving. Cu(In,Ga)Se_2 micro solar cells have achieved excellent efficiencies under concentrated light, when fabricated by materially-wasteful lithography processes. However, for commercial consideration, material-efficient synthesis approaches are required. In this work, we demonstrate a novel approach to produce arrays of Cu(In,Ga)Se_2 micro absorber layers through a two-step process, where a Cu-In-Ga precursor layer is sputtered onto a photolithographically structured resist, followed by lift-off and selenization. Our investigation shows a detrimental contamination of the Cu-In-Ga micro-dots by the photoresist. Therefore, we introduce an additional annealing step in inert-gas atmosphere prior to the selenization step, which leads to the formation of electroactive Cu(In,Ga)Se_2 micro absorbers. We report the synthesis and characterization of working micro solar cells with an efficiency of 1.2% under 1 Sun. This proof of principle opens up a new material-efficient synthesis route for the

* Corresponding authors.
E-mail addresses: Ricardo.poeira@uni.lu, Sascha.Sadewasser@inl.int (S. Sadewasser).
[1] Co-first author.

https://doi.org/10.1016/j.matdes.2023.111597

direct fabrication of arrays of micro solar cells and puts forward the potential to achieve higher power conversion efficiencies upon further process optimization.

1. Introduction

Ever since photovoltaic panels have been installed up to the year 2022, humans have deployed 1 TW of photovoltaic electricity capacity in total [1]. Approximately a further 63 TW more of photovoltaic modules are urgently required before 2050 in order to help become carbon neutral [2]. This challenge can be achieved faster if the power conversion efficiency (PCE) of photovoltaic devices can be improved since fewer materials and energy would be required. One possible way to improve efficiency is to employ light concentration which can improve the absolute efficiency of a device by 2 % per decade of illumination increase [3], i.e. a 20 % efficient device under 1 Sun, may become a 24 % efficient device under 100 Suns illumination. Recently in this context, micro-concentrator photovoltaics (micro-CPV) has gained increased attention due to its potential of surpassing standard CPV devices both in terms of cost and performance [4]. These systems are characterized by arrays of sub-millimeter solar cells in conjunction with arrays of lenses. The advantages of micro-concentrator solar cells over standard-sized (1 cm^2) CPV are material savings, better heat management, lower series resistance and enhanced efficiency [5]. Downscaling of crystalline III-V multi-junction solar cells has yielded excellent power conversion efficiencies, however edge recombination was shown to limit open-circuit voltage on cells below 1 mm^2 [6]. In contrast, thin-film polycrystalline I-III-VI_2 single junction Cu(In,Ga)Se_2 (CIGSe) solar cells have been miniaturized to 0.0025 mm^2 (squares with 50 μm side length) without suffering from edge recombination [7]. To date, large area Cu(In,Ga)(S,Se)$_2$ (CIGSSe) devices have achieved a maximum PCE of 23.4 % [8], whilst having a lower energy cost of production compared to silicon, which lowers the energy payback time and hence potential greenhouse gas emission during production, as well as raises the energy return on energy invested [9]. The synthesis comprised the magnetron sputter-deposition of a metal precursor layer followed by an annealing step introducing selenium and sulfur vapor to form the CIGSSe layer. However, the scarcity of indium and gallium might be a limiting factor for upscaling to terawatt deployment, as evidenced by their presence on the EU's scarce material list [10]. Therefore, micro-CPV based on CIGSSe is a promising approach to permit significant material savings and enhance the PCE. For example, a 100X concentration would lead to 100-fold material savings, making indium and gallium abundant again in this context.

Proof-of-concept CIGSe micro-CPV, formed from continuous large area films, yielded a solar cell with 16.3 % PCE under 1 Sun and an absolute increase of 5 % to 21.3 % PCE under 475X concentration [11]. This proof of principle has led to an increasing interest into fabricating micro solar cell arrays through material-efficient approaches using well-known and easily scalable deposition methods. Three of these approaches have been proven to work, namely, selective area electrodeposition [3,12,13], laser-based fabrication [14,15] and a physical vapor deposition method heavily modified from the standard CIGSe growth procedure [16]. In all cases, electrically active micro solar cells were synthetized, albeit with relatively low PCE. None of the above materials efficient growth techniques have made highly efficient CIGSe devices.

Here, we introduce a new synthesis design which combines the material quality of vacuum deposited materials [8] with the ability to save materials. We aim at taking advantage of the high-quality material produced by this method, whilst minimizing waste, since we sputter the Cu-In-Ga onto a patterned insulating matrix defined by photolithography. The unused sputtered material is easily separated from the removed photoresist [17,18] and recycled into new sputtering targets, which ensures a material-efficient synthesis process, unlike top-down deposition routes which removes material [7] or leaves it inactive [11]. Here we use a cheap abundant material, SiO_2, to act as an inert template to spatially separate and grow our micro-semiconductor absorber layers within it. Advantageously, the template keeps the absorber layers electrically isolated from one another without the need of deposition of an extra insulating layer, as required by some other fabrication routes [7,19].

We demonstrate this production route by fabricating arrays of 11 × 18 micro-sized CIGSe solar cells with diameters of 100 μm, making each individual cell 0.008 mm^2. The array design can easily be adjusted to the applications' needs and is scalable to industrial applications. We find that this approach leads to embedded photoresist within the precursor metal layer causing the semiconductor to release from the bottom electrode during annealing. We demonstrate a modified annealing routine to remove the photoresist and obtain flat electroactive CIGSe absorbers attached to the bottom electrode. Electrical characterization of CIGSe micro solar cell devices shows an efficiency of 1.2 % under 1 Sun.

2. Materials and methods

2.1. Fabrication

The fabrication of the CIGSe micro solar cell arrays starts with soda-lime glass substrates, onto which a 500 nm thick Mo back contact is deposited by DC magnetron sputtering. Subsequently, a 1 μm thick SiO_2 layer is deposited by chemical vapor deposition [8]. A 800 nm thick lift-off resist (LOR 5B, Kayaku Advanced Materials) and a 2 μm thick photoresist layer (AZ411, Merck) are spin coated onto the SiO_2 and a regular pattern of evenly-spaced circular areas of 100 μm diameter LORis defined by photolithography (Direct Write Laser, manufacturer). The disclosed composition of LOR 5B is 65–90 % cyclopentanone, 10–25 % 1-methoxy-2-propanol, 1–20 % polyaliphatic imide copolymer, 0.1–2 % proprietary dye B, whereas for AZ411 the composition is 2-methoxy-1-methylethyl acetate 60 % and 4-Benzoylbenzene-1,2,3-triyl tris(6-diazo-5,6-dihydro-5-oxonaphthalene-1-sulphonate 5 %. After development, reactive ion etching is employed to etch the SiO_2 layer until the Mo back contact is reached (Fig. 1a). The structured substrates, with the resist layer, are then introduced in a CIGSe sputter-deposition system (STAR: SpuTering for Advanced Research [20]), where Cu-In-Ga is deposited via DC magnetron sputtering from a single mixed target (Fig. 1b). Thus, after a lift-off process of the resist with acetone, the etched holes in the SiO_2 matrix are filled with the Cu-In-Ga (Fig. 1c). The lifted-off CIG material could be potentially separated from the resist and recycled onto CIGSe sputter targets, as in other similar processes reported recently [21].

For the pre-annealing process, the samples were placed inside a vacuum pot connected to a roughing pump and placed on a heating plate (Fig. 1d). To ensure minimum oxygen content inside the pot, three cycles of nitrogen purging and pumping were performed prior to heating up. Separately, a heating plate is set to 440 °C

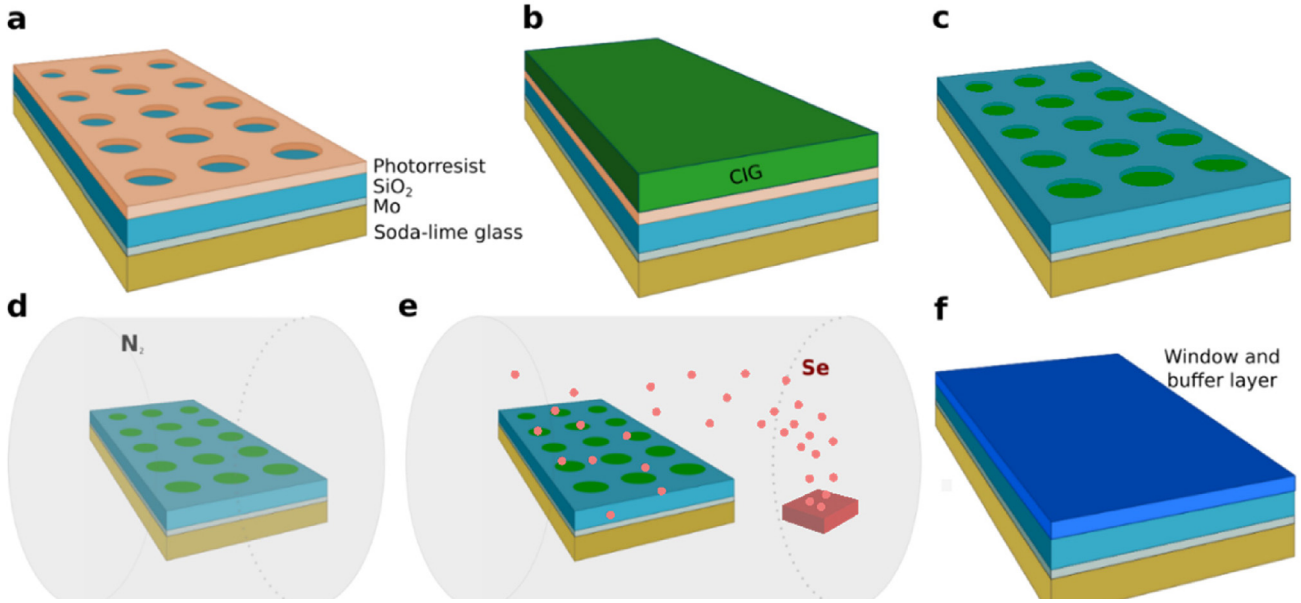

Fig. 1. Schematic representation of the different steps involved in the synthesis process of CIGSe micro solar cell arrays: a) creation of the SiO_2 holes by photolithography and etching process. b) Deposition of Cu-In-Ga metallic precursor and c) removal of photoresist and excess Cu-In-Ga. d) Pre-annealing of the array inside a nitrogen-containing chamber and e) subsequent selenization of the Cu-In-Ga metallic precursor by elemental selenium evaporation to form CIGSe absorber. f) Micro solar cell stack after deposition of CdS buffer and ZnO/ZnO:Al window layers.

and once the set temperature is reached, the vacuum pot is placed on the heating plate for 20 min. The vacuum pot is kept at 400 mbar during the annealing routine. After the pre-annealing period, the pot is removed from the heating plate and left to cool down to room temperature.

The selenization step was conducted in a quartz tube oven with a closed graphite box containing both the micro-precursors as well as 150 mg of selenium powder (Fig. 1e). Three cycles of nitrogen purging and pumping were performed to minimize oxygen inside the tube. The tube was then refilled with nitrogen to 350 mbar before the annealing procedure was initiated. The quartz tube was heated up to 465 °C with a heating ramp of 17 °C/min, followed by a 10-minute period at constant temperature, after which the system is let to cool down to room temperature.

The CIGSe micro absorbers were etched in a 10 wt% KcN aqueous solution for one minute, directly followed by the deposition of a 50 nm CdS buffer layer through chemical bath deposition [22]. The window layers, intrinsic ZnO (50 nm) and Al-doped ZnO (400 nm), were deposited by radio-frequency magnetron sputtering (Fig. 1f).

2.2. Characterization

Optical images and height maps were measured with a confocal laser scanning microscope (CLSM, Keyence VK-X1000) equipped with an UV laser (404 nm). Scanning electron microscopy (SEM) micrographs were captured with a Zeiss EVO10 microscope coupled with an UltimMax40 detector allowing for energy dispersive X-ray spectroscopy (EDX) analysis.

Photoluminescence images of the micro-absorber arrays were acquired with an intensity-calibrated home-built setup using a 532 nm excitation laser, a laser beam homogenizer, an InGaAs detector array and optical objectives. Raman spectroscopy was performed using a 532 nm laser excitation in conjunction with a 2400 lines/mm grating and a Renishaw inVia micro-Raman spectrometer. External quantum efficiency (EQE) measurements on individual micro-absorbers were acquired on a home-built setup calibrated with silicon and InGaAs photodiodes. Nevertheless, since the illumination spot is larger than the single micro-dot's surface area, only semi-quantitative EQE could be extracted. Groups of up to 23 micro solar cells were electrically isolated by mechanical scribing. Current-voltage curves were measured under AM1.5 illumination using an AAA class solar simulator.

3. Results and discussion

3.1. Investigation of micro-precursors

To assess the homogeneity and reproducibility of the sputtered Cu-In-Ga micro-precursors, we measure the morphology of individual micro-dots, through optical sectioning with a confocal laser scanning microscope (CLSM), as shown in Fig. 2a and b. On average, all precursors show a diameter of 100 ± 1 μm and have a similar (±3%) protruding height compared with the SiO_2 matrix. Furthermore, the precursors show a flat and smooth surface with a narrow rim (1–2 μm width) along the perimeter, which is protruding higher (0.2–0.4 μm) than the inner region of the dot, as visible in the height map. To investigate the origin of the rim, cross-section SEM images were acquired before the resist removal (Fig. 2c). As expected, the sputtered Cu-In-Ga covers the complete substrate, filling in the empty dots. However, focusing on the edge of the micro-dot (red box in Fig. 2c), we observe that a small part (1.5 μm) of the SiO_2 layer is neither covered by the resist nor by the Cu-In-Ga, suggesting that the resist was damaged and removed during the Cu-In-Ga sputtering. Given that this length coincides with the width of the protruding rim observed by CLSM, it is possible that its origin is related to the abrasion of the resist during the sputtering of the metallic precursor, causing an accumulation of Cu-In-Ga deposit along the edge between the resist and the micro-dot. This would imply that the protruding rim is a blend of Cu-In-Ga and organic resist. If this resist damage occurs throughout the sputtering process filling up the micro-dot, the incorporation of resist within the Cu-In-Ga precursor is not limited to the surface, but might affect the whole micro-dot volume. Note that damages to photolithography resists by magnetron sputtering processes have been previously reported [23]. Further analyses, sup-

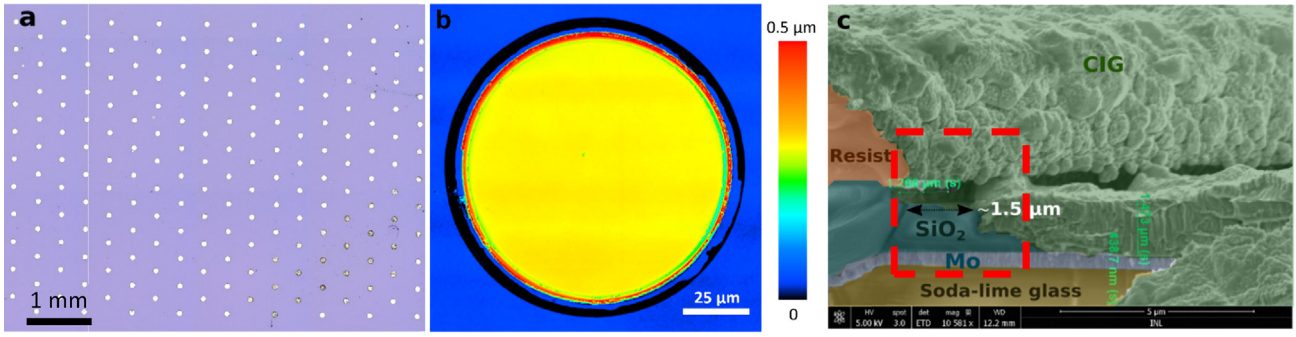

Fig. 2. A) optical image of an array of cu-in-ga-filled dots. b) clsm height map of a close-up on a single micro-precursor. c) sem cross-section image of a micro-dot before resist removal (the colors are added for clarity). red dashed box indicates region without resist nor cu-in-ga. (For interpretation of the references to colour in this figure legend, the reader is referred to the web version of this article.)

porting the presence of carbon-based resist within the Cu-In-Ga precursor, are discussed in the Supplementary Information (SI) section S1.

The properties of CIGSe absorber layers heavily depend upon their elemental composition [24]. EDX analysis showed a homogeneous composition at the array level, as well as within a single precursor, with the two important characteristic ratios $CGI = [Cu]/([Ga] + [In]) = 1.4 \pm 0.2$ and $GGI = [Ga]/([Ga] + [In]) = 0.5 \pm 0.1$. We note that the EDX's electron beam scan resulted in a localized inflation of the Cu-In-Ga precursor layer, which we associate with the resist contamination mentioned previously (further details given in the SI section S2).

3.2. Metal precursor annealing

At this stage of the synthesis, the selenization annealing step converts the Cu-In-Ga precursor into the CIGSe absorber. However, directly selenizing the as-produced precursors consistently resulted in the delamination of the CIGSe absorbers, as discussed later. Combining the recurrent delamination with the analysis of the precursor's cross-section images, we hypothesize that, during the sputtering process, fractions of the resist are incorporated inside the micro-dot along with the Cu-In-Ga precursor, later causing the observed undesired deformation during the annealing step (and EDX measurements). Therefore, we introduced an additional pre-annealing step in the fabrication process, performed in inert atmosphere, with the goal to extract the resist contaminants prior to the selenization process. In the following, we compare two arrays of micro-dots, processed (I) by a direct selenization treatment (annealing in a selenium-containing atmosphere), where the vaporization of contaminants and the selenization take place simultaneously, and (II) by a pre-annealing step in inert atmosphere, followed by the selenization step.

To assess the pre-annealing step, we compare the morphology of the precursor before and after the pre-annealing treatment by SEM and CLSM characterization (see Fig. 3). The as-deposited precursors are characterized by a flat, smooth and compact morphology with a rim along the perimeter. Conversely, the pre-annealed precursors present a rougher surface, marked by an apparently porous and granular morphology. In particular, part of the rim along the perimeter has disappeared due to the pre-annealing treatment, in agreement with the hypothesis of the blend of Cu-In-Ga and resist. EDX mapping, shown in SI section S1, confirms a higher carbon content along the rim, whose vaporization during the pre-annealing process would explain the deformation of the rim. According to the phase diagrams of CuGa and CuIn [25,26], both show a liquid phase at temperatures above 300 °C, meaning that the pre-annealing is partly melting the precursor. At 440 °C, the organic resist is expected to vaporize and degas out of the partially liquid Cu-In-Ga matrix, resulting in a porous morphology upon cooling down to room temperature. To confirm the influence of the resist, a normal large-area Cu-In-Ga precursor was sputtered without the use of any photoresist and the respective pre-annealing did not result in a porous morphology, as shown in SI section S3.

The as grown and the pre-annealed arrays were subsequently selenized in identical conditions (Fig. 4a and c, respectively). The selenization of the as grown precursors consistently resulted in heavily deformed absorbers, as illustrated by the height map in Fig. 4b. We expect the CIGSe absorber to be roughly double the thickness of its precursor due to the expansion of incorporating selenium, meaning we anticipate a CIGSe thickness of about 2 µm for the micro-dots. However, the measured volume expansions of the directly selenized precursors suggest more than a 20-fold increase in thickness. Since the absorber retains its diameter (100 µm), the obtained morphology/volume cannot be compact and must be mostly hollow, which compromises the electrical contact between the absorber and the molybdenum back contact layer. In fact, these microscopic expansions are visible in a 45° SEM measurement (shown in SI section S4), where the detachment of the absorber layers is perceptible. Although the details of the underlying expansion mechanism are not clear, we suggest that during the annealing, the presence of selenium causes the formation of an impermeable solid CIGSe phase at the surface, whilst the high temperatures cause the vaporization of the underlying organic contaminants, which cannot easily escape. The resulting trapped vapors cause an upward pressure on the CIGSe crust that leads to the deformation of the absorber.

The introduction of the pre-annealing step has the objective of extracting the contaminants that we hypothesize for being responsible for the abnormal expansion of the CIGSe absorbers. As shown in Fig. 4d, absorbers that were pre-annealed in inert atmosphere and subsequently selenized display a morphology with a thickness around the expected value of 2 µm, suggesting that a compact film was achieved. A closer analysis puts forward a three-dimensional expansion, as the diameter of the selenized film is (12 ± 4)% larger compared to its precursor. To better understand this lateral expansion, EDX measurements were performed radially from the center of the dot to the SiO_2 insulating matrix, spatially resolving the silicon signal (Fig. 4e). The silicon signal remains constant outside the micro-dot's original diameter (i.e. micro-dot's aura) and drops abruptly to zero within it. Therefore, we confirm a muffin-top growth of the CIGSe absorber (illustrated in Fig. 4f), rather than a deformation of the SiO_2 by the lateral expansion of the CIGSe. However, the distribution of Ga in the absorber is not identical in these two regions, as shown in Fig. 4e through the

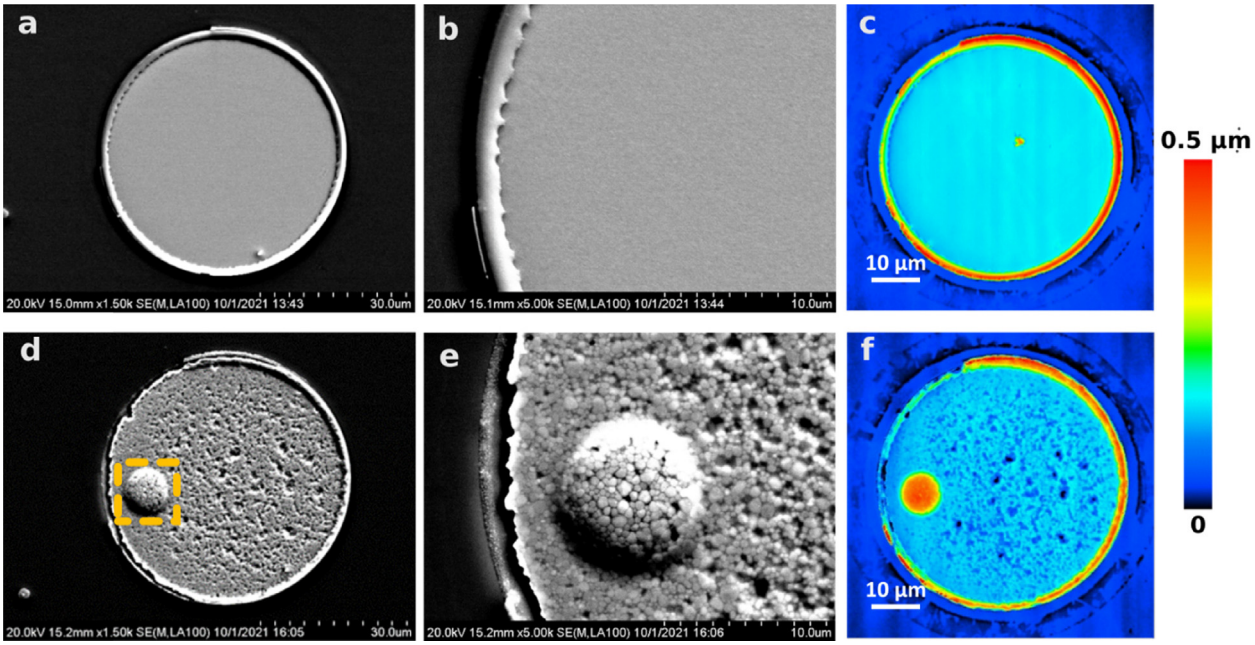

Fig. 3. Comparison of the precursor's morphology: a-c) before and d-f) after the pre-annealing treatment. a-b) and d-e): SEM images of the Cu-In-Ga precursor. The circular dome visible in the pre-annealed micro-dot originates from an EDX area-spectrum measurement taken before pre-annealing within the area designated by the orange dashed box (see Fig. 2d in SI). c) and f) CLSM height maps of the same micro-precursor. (For interpretation of the references to colour in this figure legend, the reader is referred to the web version of this article.)

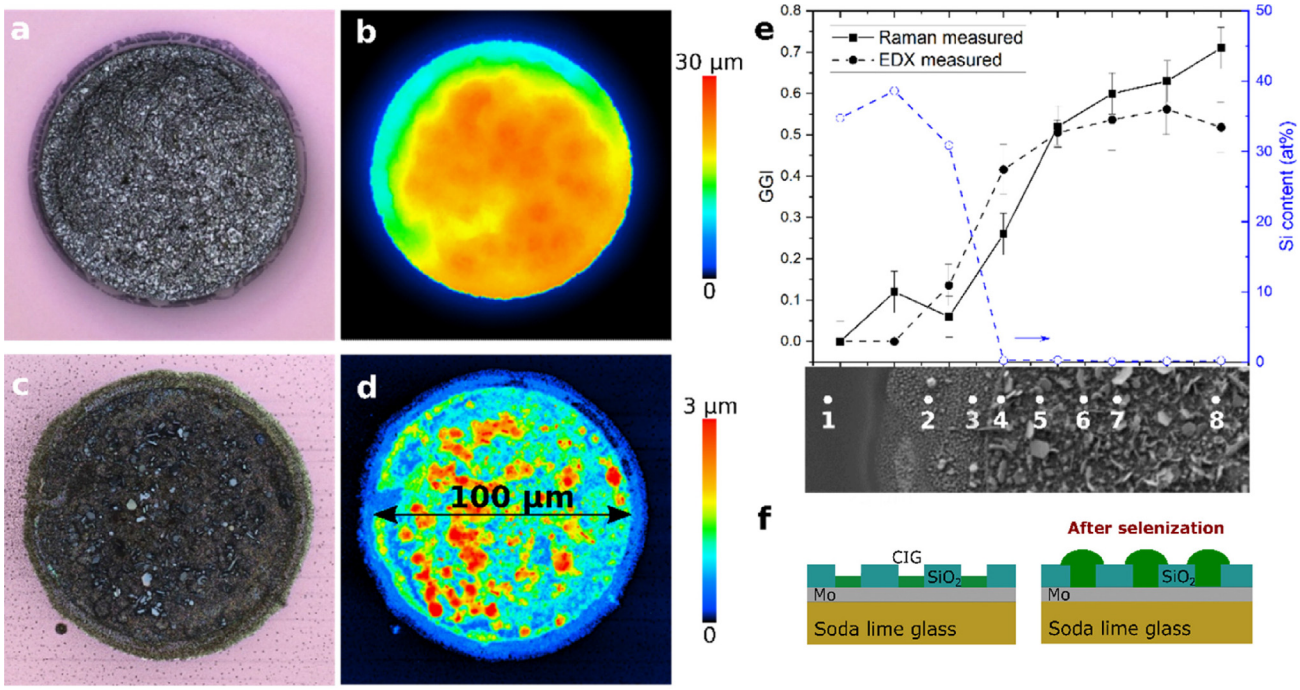

Fig. 4. CLSM optical image and respective height map of: a-b) direct selenization of the micro-precursor; here only expansion in the z-direction is observed, with an unchanged 100 µm diameter; c-d) pre-annealing followed by selenization of the micro-precursor, where expansion in 3D is noted. e) Compositional ratio GGI and silicon content as a function of position across the micro-absorber. Measurements start on the SiO_2 matrix and proceed towards the center of the dot. A schematic cross section representation of the sample geometry before and after selenization is given in f).

$GGI = [Ga]/([Ga] + [In])$ compositional ratio. The spatially resolved EDX and Raman analysis, both corroborate that no/very low amount of Ga is detected within the aura of the micro-dot. This leads us to believe the chalcopyrite phase that "flows" outside of the dot, and forms the aura, is $CuInSe_2$. Mainz et al. have shown that during selenization, In tends to migrate to the surface, causing Ga to segregate at the back of the absorber [27]; here, we speculate that the lateral diffusion of In hinders the diffusion of Ga towards the aura.

It is worth noting that all micro-dots within the same array show a similar absorber expansion, however the selenization of some pre-annealed arrays have also yielded delaminated absor-

bers. Nevertheless, statistically, 60 % of the pre-annealed samples were successfully selenized compared to 0 % of the micro-dots selenized without pre-annealing. Despite not being able to pinpoint the reason for not having 100 % success rate, we suggest, that depending on the initial amount of contaminants within the micro-dots, longer pre-annealing times are required to degas the resist from the Cu-In-Ga precursors.

To summarize the findings from our annealing/selenization study of Cu-In-Ga micro-precursors deposited by magnetron sputtering, we can state that (I) direct selenization of the precursor leads to abnormal expansion and/or delamination of all absorber dots, which we attribute to the incorporation of resist within the Cu-In-Ga precursor; and (II) pre-annealing of precursors in nitrogen followed by selenization yielded the expected absorber morphology. Our results show that the additional pre-annealing step was necessary to remove the resist incorporated in the precursor.

3.3. Absorber quality control and device characterization

In the following, we discuss the characterization of micro-absorbers that were converted into micro solar cells. Our micro-absorbers contain an excess of copper ($CGI = 1.4$), which has been shown to give better carrier transport properties to the resulting absorbers [24]. However, the excess of copper implies that, during the selenization step, the secondary phase copper selenide (Cu_2Se) as well as the CIGSe chalcopyrite phase are formed. This secondary phase is a degenerate semiconductor that acts as a recombination center, resulting in shunted solar cells [28]. Furthermore, solar cells with excess copper are reported to be dominated by interface recombination [24], which results in a decrease of the quasi-fermi level splitting and ultimately a lower power conversion efficiency. To overcome these issues, a standard KcN (10 wt% for 5 min) treatment is applied to the array, directly followed by the chemical bath deposition of a 50 nm CdS buffer layer. The former is aimed at removing the copper selenide secondary phases from the micro-absorbers and the CdS buffer layer to improve the CIGSe interface.

To assess the optoelectronic quality of the micro-absorbers in the array, photoluminescence and external quantum efficiency (EQE) measurements were performed. Since the photoluminescence setup is intensity calibrated, we can extract the photoluminescence quantum yield (PLQY) of our micro-absorbers. PLQY is defined as the ratio of the absorber's photoluminescence, originating from radiative recombination, and the photon flux impinging on the absorber [29]. It contains information about the fraction of radiative recombination and thus the quality of the absorber. Fig. 5a shows a CLSM optical image of a fraction of an array of micro solar cells. The corresponding spatially-resolved panchromatic PLQY map, as well as a zoomed-in PLQY map are shown in Fig. 5b and c. The PLQY is inhomogeneous, when comparing the different micro solar cells. Given that the precursors were grown with an excess of copper, we assume that shunting, caused by persistent copper selenide secondary phases within the CIGSe semiconductor layer itself, is responsible for this inhomogeneity. Furthermore, focusing at the level of a single dot, it appears that the aura of some dots luminesces more than their central region. Given that the Ga-containing CIGSe phase (center of the dots) is characterized by a larger bandgap than that of the CISe aura [30], the PLQY maps also imply that the aura should lead to a higher open-circuit voltage compared to the center of the dots.

From semi-quantitative EQE spectra on individual micro-absorbers (Fig. 6a), the average bandgap is estimated to $E_{gap}^{EQE} = (1.3 \pm 0.1)eV$. This value agrees well with the bandgap $E_{gap}^{Exp} = (1.3 \pm 0.2)eV$ calculated empirically from the GGI of our metal precursors ($GGI = 0.46$) [31], which agrees with our experimental estimation. From the general shape of the EQE spectrum, we identify a poor carrier collection in the infrared range above the bandgap. Furthermore, we associate the drop in the UV-region to parasitic absorption by the CdS buffer layer, which may be too thick, given that the chemical deposition method was not optimized for micro-absorbers.

To have an estimation of the number of successfully made solar cells we probed each cell with the EQE beam set to 532 nm and measured the resulting current. From the possible 198 solar cells, 182 were found to produce current, with 55% of the active cells showing at least half of the highest current measured in the array. To perform a more complete characterization, current–voltage (JV) measurements on the array of micro solar cells, we electrically isolated groups of dots to minimize the risk of a shunt. Fig. 6b shows the JV characteristics of a pair of isolated micro solar cells. The devices show a diode-like behavior with a PCE of $(1.2 \pm 0.3)\%$ under 1 Sun. JV characteristics of arrays with 14 and 23 micro solar cells are shown in Figure S5 in the SI. The short circuit current density, Jsc, is found to be $14 \pm 2 mA/cm^2$ which is in line with the EQE showing very poor collection in the near-infrared region. The active area considered for the JV measurements was given by the number of micro solar cells in the respective group multiplied by the area of a 50 μm radius disc, which is the area within the SiO_2 template where the absorber layer is grown. A detailed discussion of the active area is given in the SI. It is evident that these micro solar cells suffer from a high series resistance, which could be improved by optimizing the CdS buffer deposition and the implementation of appropriate top contact collection grids. On the other hand, the voltage-dependent current collection shows that the

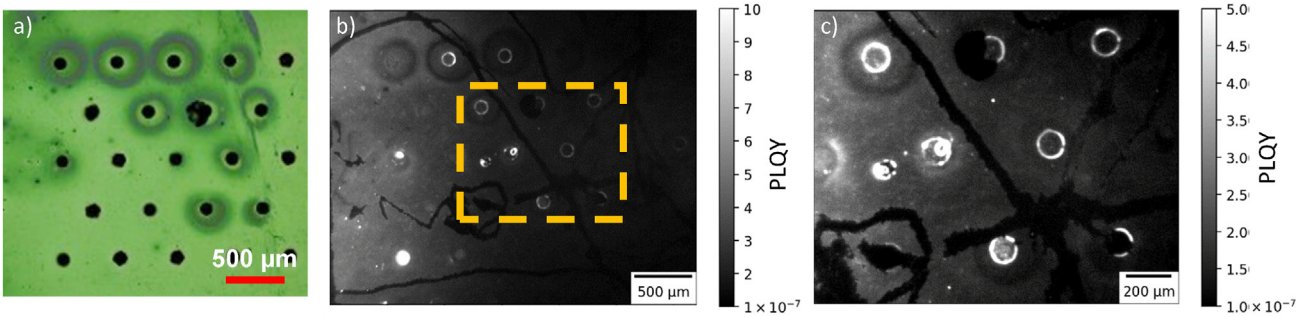

Fig. 5. A) clsm optical image of a fraction of the array area where plqy map is measured in 5b. image was taken after buffer and window layers' deposition but prior to the scribing for electrical insulation. b) panchromatic plqy map of the array of micro-absorbers. darker lines on plqy map are due to scribing lines, done prior to the measurement. orange dashed square shows region where zoomed-in plqy map, shown in 5c, was measured. c) zoomed-in pl map onto micro-absorbers showing a higher plqy along the aura compared to their center. (For interpretation of the references to colour in this figure legend, the reader is referred to the web version of this article.)

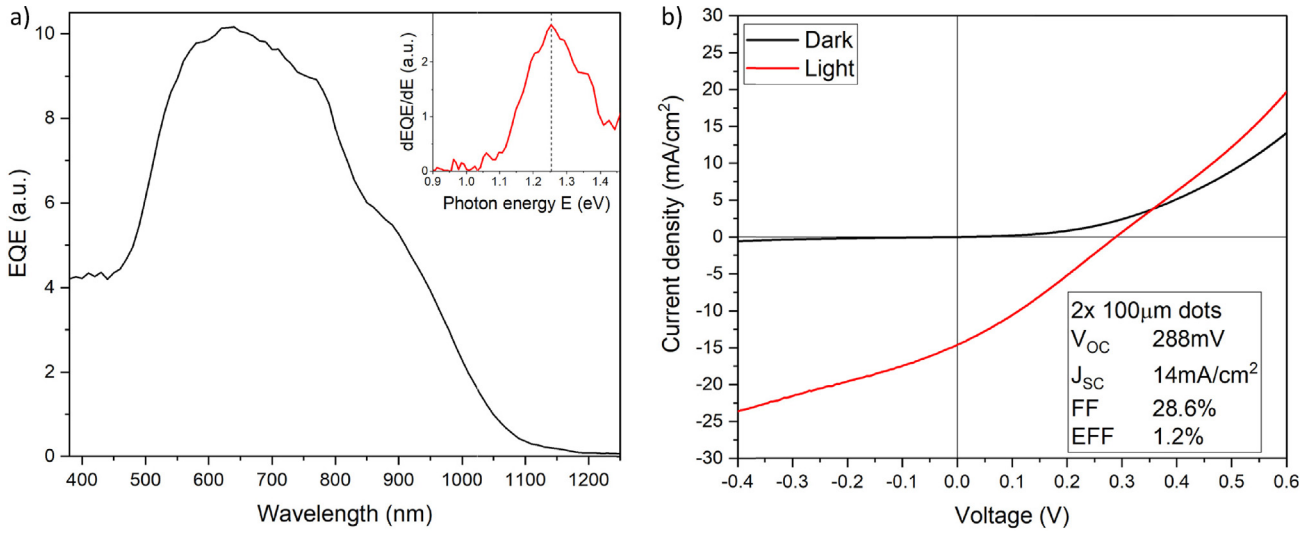

Fig. 6. A) semi-quantitative eqe measurement on one micro solar cell, with the respective energy derivative as inset to determine the bandgap. eqe units are a.u. because the laser beam size was larger than the micro-absorber active area. b) jv characteristics of an electrically isolated group of two micro solar cells connected in parallel.

shunt resistance is deteriorating the device performance. This is likely related to shunt paths resulting from the excess of copper of the precursors. Both causes can help explain the relatively low open-circuit voltage and fill factor. Nonetheless, our results provide a first proof of concept for the production of arrays of micro solar cells through a combined sputtering lithography approach.

4. Conclusion

In this work, we show a proof of principle for the synthesis of arrays of micro solar cells grown by a material-efficient method where metal precursors are sputtered into an earth-abundant patterned SiO_2 matrix and subsequently annealed to form CIGSe micro-absorbers. A comparison between two annealing routines has proven that a two-step annealing is necessary to produce working solar cells, which we associate with the resist contaminants from the sputtering process. Proof-of-concept micro solar cells displayed an efficiency of 1.2 % under 1 Sun, which is expected to significantly increase upon concentration. Our approach opens up a synthesis route to optimize and improve the PCE of material efficient processed micro solar cells. In future work, we aim to significantly improve the efficiency values by optimizing the buffer layer for micro solar cells and by depositing Cu-poor CIGSe absorbers. The chosen mini-module SiO_2 matrix design is flexible since the dimensions and pattern of the cells can be adjusted for a wide variety of light concentrations and optical geometries. Moving forward, using micro optics in-conjunction with micron sized thin film absorber layers enables indium and gallium to be considered as earth abundant for use in thin film photovoltaics and therefore offers a possible pathway to terawatt deployment.

Data availability

Data will be made available on request.

Declaration of Competing Interest

The authors declare that they have no known competing financial interests or personal relationships that could have appeared to influence the work reported in this paper.

Acknowledgements

The authors acknowledge Michele Melchiorre for buffer and window layers deposition. Pedro Anacleto is acknowledged for helpful discussions.

This research was funded in part by the Luxembourg National Research Fund (FNR), grant reference [PRIDE17/12246511/PACE]. The authors acknowledge additional support by the "Micro-concentrator thin film solar cells (MiconCell)" project (PTDC/CTM-CTM/28922/2017) co-funded by FCT and ERDF through COMPETE2020. Marina Alves thanks the Fundação para a Ciência e a Tecnologia (FCT), Portugal for the PhD Grant (2020.06063.BD).For the purpose of open access, the author has applied a Creative Commons Attribution 4.0 International (CC BY 4.0) license to any Author Accepted Manuscript version arising from this submission.

Appendix A. Supplementary data

Supplementary data to this article can be found online at https://doi.org/10.1016/j.matdes.2023.111597.

References

[1] S. Philipps and W. Warmuth, Photovoltaics Report. (2022). [Online]. Available: https://www.ise.fraunhofer.de/content/dam/ise/de/documents/publications/studies/Photovoltaics-Report.pdf.
[2] D. Bogdanov et al., Low-cost renewable electricity as the key driver of the global energy transition towards sustainability, Energy 227 (2021), https://doi.org/10.1016/j.energy.2021.120467 120467.
[3] D. Siopa et al., Micro-sized thin-film solar cells via area-selective electrochemical deposition for concentrator photovoltaics application, Sci. Rep. 10 (2020) 14763, https://doi.org/10.1038/s41598-020-71717-0.
[4] M. Paire, L. Lombez, J.-F. Guillemoles, D. Lincot, Toward microscale Cu(In, Ga) Se2 solar cells for efficient conversion and optimized material usage: Theoretical evaluation, J. Appl. Phys. 108 (2010), https://doi.org/10.1063/1.3460629 034907.
[5] M. Alves, A. Pérez-Rodríguez, P.J. Dale, C. Domínguez, S. Sadewasser, Thin-film micro-concentrator solar cells, J. Phys. Energy 2 (2019), https://doi.org/10.1088/2515-7655/ab4289 012001.
[6] P. Albert et al., Miniaturization of InGaP/InGaAs/Ge solar cells for micro-concentrator photovoltaics, Prog. Photovoltaics Res. Appl. 29 (2021) 990–999, https://doi.org/10.1002/pip.3421.
[7] M. Paire et al., Cu(In, Ga)Se 2 mesa diodes for the study of edge recombination, Thin Solid Films 582 (2015) 258–262, https://doi.org/10.1016/j.tsf.2014.11.033.
[8] M. Nakamura, K. Yamaguchi, Y. Kimoto, Y. Yasaki, T. Kato, and H. Sugimoto, Cd-Free Cu(In,Ga)(Se,S) 2 Thin-Film Solar Cell With Record Efficiency of 23.35%,

IEEE J. Photovoltaics, 9 (2019), pp. 1863–1867, 10.1109/JPHOTOV.2019.2937218.
[9] M. Arguelles, N. Bennet, and C. D. Daniels, UNDP global environmental finance unit annual performance report. (2016). [Online]. Available: https://www.undp.org/sites/g/files/zskgke326/files/publications/2016 APR UNDP-GEF final.pdf.
[10] G.A. Blengini et al., Study on the EU's list of critical raw materials. (2020), https://doi.org/10.2873/24089.
[11] M. Paire et al., Cu(In, Ga)Se2 microcells: High efficiency and low material consumption, J. Renew. Sustain. Energy 5 (2013) 1–6, https://doi.org/10.1063/1.4791778.
[12] S. Sadewasser, P.M.P. Salomé, H. Rodriguez-Alvarez, Materials efficient deposition and heat management of CuInSe2 micro-concentrator solar cells, Sol. Energy Mater. Sol. Cells 159 (2017) 496–502, https://doi.org/10.1016/j.solmat.2016.09.041.
[13] A. Duchatelet, K. Nguyen, P.-P. Grand, D. Lincot, M. Paire, Self-aligned growth of thin film Cu(In, Ga)Se2 solar cells on various micropatterns, Appl. Phys. Lett. 109 (2016), https://doi.org/10.1063/1.4971975 253901.
[14] F. Ringleb et al., Locally grown Cu(In, Ga)Se2 micro islands for concentrator solar cells, in *Physics*, Simulation, and Photonic Engineering of Photovoltaic Devices VII 2018 (10527) (2018) 7, https://doi.org/10.1117/12.2288253.
[15] B. Heidmann et al., Fabrication of Regularly Arranged Chalcopyrite Micro Solar Cells via Femtosecond Laser-Induced Forward Transfer for Concentrator Application, ACS Appl. Energy Mater. 1 (2018) 27–31, https://doi.org/10.1021/acsaem.7b00028.
[16] B. Heidmann et al., Local growth of CuInSe 2 micro solar cells for concentrator application, *Mater. Today*, Energy 6 (2017) 238–247, https://doi.org/10.1016/j.mtener.2017.10.010.
[17] 渊上真一郎, 山口典生, 爰甲雅彦, 清水巧治, and 竹泽浩乂, Photoresist stripping solution, stripping solution recycling system and operating method, and method for recycling stripping solution, CN103688222A, 2011 [Online]. Available: https://patents.google.com/patent/CN103688222A/en.
[18] 魏任重, 徐雅玲, 黄源, 尹云舰, and 连杰, Method for recovering waste photoresist stripper, CN102951761A, 2012 [Online]. Available: https://patents.google.com/patent/CN102951761A/en.
[19] M. Paire et al., Resistive and thermal scale effects for Cu(In, Ga)Se2 polycrystalline thin film microcells under concentration, Energy Environ. Sci. 4 (2011) 4972, https://doi.org/10.1039/c1ee01661j.
[20] D. Fuster et al., System for manufacturing complete Cu(In, Ga)Se2 solar cells in situ under vacuum, Sol. Energy 198 (2020) 490–498, https://doi.org/10.1016/j.solener.2020.01.073.
[21] D. Hu, B. Ma, X. Li, Y. Lv, Y. Chen, C. Wang, Innovative and sustainable separation and recovery of valuable metals in spent CIGS materials, J. Clean. Prod. 350 (2022), https://doi.org/10.1016/j.jclepro.2022.131426 131426.
[22] M. Sood et al., Absorber composition: A critical parameter for the effectiveness of heat treatments in chalcopyrite solar cells, Prog. Photovoltaics Res. Appl. 28 (2020) 1063–1076, https://doi.org/10.1002/pip.3314.
[23] S. M. Rossnagel, D. Mikalsen, H. Kinoshita, and J. J. Cuomo, Collimated magnetron sputter deposition, *J. Vac. Sci. Technol. A Vacuum, Surfaces, Film.*, 9 (1991), pp. 261–265, 10.1116/1.577531.
[24] S. Siebentritt, L. Gütay, D. Regesch, Y. Aida, V. Deprédurand, Why do we make Cu(In, Ga)Se2 solar cells non-stoichiometric?, Sol Energy Mater. Sol. Cells 119 (2013) 18–25, https://doi.org/10.1016/j.solmat.2013.04.014.
[25] Z. Bahari, E. Dichi, B. Legendre, J. Dugué, The equilibrium phase diagram of the copper–indium system: a new investigation, Thermochim. Acta 401 (2003) 131–138, https://doi.org/10.1016/S0040-6031(02)00500-2.
[26] C.-S.-J.-H. Suryanarayana, Mechanism of low-temperature θ -CuGa2 phase formation in Cu-Ga alloys by mechanical alloying, J. Appl. Phys. 96 (2004) 6120–6126, https://doi.org/10.1063/1.1808243.
[27] R. Mainz et al., Time-resolved investigation of Cu(In, Ga)Se 2 growth and Ga gradient formation during fast selenisation of metallic precursors, Prog. Photovoltaics Res. Appl. 23 (2015) 1131–1143, https://doi.org/10.1002/pip.2531.
[28] T.-P. Hsieh, C.-C. Chuang, C.-S. Wu, J.-C. Chang, J.-W. Guo, W.-C. Chen, Effects of residual copper selenide on CuInGaSe2 solar cells, Solid. State. Electron. 56 (2011) 175–178, https://doi.org/10.1016/j.sse.2010.11.019.
[29] P. Caprioglio et al., On the Relation between the Open- Circuit Voltage and Quasi-Fermi Level Splitting in Efficient Perovskite Solar Cells, Adv. Energy Mater. 9 (2019) 1901631, https://doi.org/10.1002/aenm.201901631.
[30] J.-C. Park, J.-R. Lee, M. Al-Jassim, T.-W. Kim, Bandgap engineering of Cu(In_1-xGa_x)Se_2 absorber layers fabricated using CuInSe_2 and CuGaSe_2 targets for one-step sputtering process, Opt. Mater. Express 6 (2016) 3541, https://doi.org/10.1364/OME.6.003541.
[31] W. Witte et al., Gallium gradients in Cu(In, Ga)Se 2 thin-film solar cells, Prog. Photovoltaics Res. Appl. 23 (2015) 717–733, https://doi.org/10.1002/pip.2485.